Photorefractivity in a functional side-chain polymer

B. Kippelen,* K. Tamura,† and N. Peyghambarian
Optical Sciences Center, University of Arizona, Tucson, Arizona 85721

A. B. Padias and H. K. Hall, Jr.
Chemistry Department, University of Arizona, Tucson, Arizona 85721
(Received 12 February 1993)

An experimental study of the photorefractive effect in a polymeric material containing carbazole and the second-order tricyanovinylcarbazole moieties as a side chain is presented. This polymeric system exhibits intrinsically both photoconductivity and the electro-optic effect. Absorptive and photorefractive gratings have been evidenced by four-wave-mixing experiments and electro-optic measurements. The properties of the photorefractive gratings are studied by investigating the electric-field dependence of the diffraction efficiency. The dynamics of the erase-write behavior of the gratings, as well as permanent photobleaching of the polymer, are described.

I. INTRODUCTION

Photorefractive materials are of particular importance because they exhibit a reversible refractive index change under a low-power laser-beam illumination. They can therefore be used as versatile storage media for erasable read-write optical memories or as reconfigurable interconnects.[1] The photorefractive (PR) effect has been evidenced and studied the past two decades mostly in inorganic materials such as ferroelectrics ($LiNbO_3$, $BaTiO_3$, $LiTaO_3$, etc.), sillenites (BSO, BGO, BTO, etc.), or doped semiconductors (GaAs:Cr, InP:Fe, etc.). The optimization of the efficiency of these inorganic crystals for photorefractive applications suffers from the fact that high electro-optic (EO) coefficient r is accompanied by a high dc dielectric constant ε, limiting the commonly used figure of merit for the PR effect ($n^3 r/\varepsilon$). Recently, the PR effect has been evidenced in an organic crystal[2] and in polymeric materials.[3–6] Organic materials for photorefractive applications are of great interest because they exhibit large EO coefficients, have a low dielectric constant, and can be functionalized and easily processed at low cost into a rich variety of thin films and waveguides.

To be photorefractive, a polymer needs to have second-order nonlinear optical properties in addition to photoconductivity. Photorefractivity has been demonstrated so far in guest-host systems[3–6] where a glassy polymer matrix is doped with either a transport agent for the photoconductivity, a photosensitizer or a second-order molecule (NLO chromophores). The electro-optic effect due to alignment of the chromophores is achieved by applying a field to the sandwich formed by the polymer placed between two electrodes or by Corona poling. The guest-host approach leads to a polymeric system with a low glass transition temperature T_g and consequently low stability. Here, we report photorefractivity in a side chain polymeric material[7] which has both the photoconductivity and the electro-optic effect intrinsically. This approach can lead to high-T_g polymers. Modified polyvinylcarbazole (PVK) was used as starting material since it is well known for its photoconductive properties.[8–11] A portion of the carbazole groups were reacted with tetracyanoethylene to form tricyanovinylcarbazole (TCVK) groups which have second-order properties. The nonlinear chromophores, in this case, are attached to the backbone as a side chain and higher stability of the electro-optic effect is obtained.[7] But in return for better stability, high poling fields are needed (100 V/μm). This high value restrains the thickness of the samples that can be poled efficiently and limits therefore the interaction length in diffraction experiments unless the sample is used in a waveguide configuration.

In this paper, we report the observation of photorefractivity in a carbazole-tricyanovinylcarbazole (PVK-TCVK) polymeric system, modified in order to ease the poling process of thick samples. Four-wave mixing and Mach-Zehnder–type experiments were performed and the diffraction efficiency was measured as a function of the applied field. The erase-write properties of the gratings and their dynamics are discussed as well. Finally, we show that the polymer can exhibit some permanent photobleaching of the absorption and related refractive index changes due to photochemical reactions of the polymer when it is excited close to its absorption band. This photobleaching process lowers permanently the refractive index at wavelengths greater than 500 nm.

II. THEORETICAL BACKGROUND

The formation of a photorefractive grating can be a complex process and therefore its theoretical description is still the subject of active research. However, the model introduced by Kukhtarev and co-workers[12–16] has provided a solid framework for the description of the formation of a photorefractive grating and appears to agree reasonably well with experimental results obtained in inorganic crystals. The Kukhtarev model does not take into account the physics of photocarrier generation and

recombination for which a model has been presented by Onsager.[17] A first-order approximation of this geminate recombination process has been introduced into the Kukhtarev model by Twarowski[18] to describe the photorefractive grating formation in organic crystals and polymers. Hole photogeneration studies[11] in PVK show that an external applied field plays an important role in the generation of photocarriers. Therefore, to describe the photorefractivity in our material, we will apply the simple Kukhtarev model in the steady state including Onsager geminate recombination and modified to take into account the field dependence of the electro-optic coefficient.

In photorefractive crystals, the interference of two coherent writing beams leads to a periodic light intensity distribution that causes photoexcitation of mobile charge carriers. These photogenerated carriers migrate by diffusion, or by drift when an external field is applied along the grating vector, and are trapped at new sites. This charge transport induces a periodic space-charge distribution and consequently a space-charge field. This results in a refractive index modulation through the space-charge field and the electro-optic effect. In the steady state, the amplitude of the electro-optic photorefractive index modulation Δn_{eo} is expressed as

$$\Delta n_{eo}=\tfrac{1}{2}n^3 r_{eff}E_{sc} , \tag{1}$$

where n is the background refractive index and r_{eff} is the effective electro-optic coefficient which depends on the symmetry of the sample and the experimental configuration. The amplitude of the space-charge field E_{sc} is given by

$$E_{sc}=\left[\frac{(E_0^2+E_D^2)}{(1+E_D/E_q)^2+(E_0/E_q)^2}\right]^{1/2} . \tag{2}$$

E_0 is the component of the external applied field along the grating vector. The diffusion field E_D is defined as

$$E_D=\frac{Kk_BT}{e} , \tag{3}$$

where K is the grating vector, k_B is the Boltzmann constant, T the temperature, and e the elementary charge. In Eq. (2), the trap-limited field E_q is given by

$$E_q=\frac{eN_A}{K\varepsilon\varepsilon_0} . \tag{4}$$

ε is the dc dielectric constant, ε_0 the permittivity, and N_A the density of photorefractive traps. Equations (2)–(4) show that the space charge increases when an external field is applied and tends to a saturation value that is mainly limited by the density of photorefractive traps. The field dependence of a photorefractive signal is therefore a basic signature of the electro-optic photorefractive effect. Another essential feature and property of photorefractivity is the nonlocal response, i.e., the phase shift Ψ between the space-charge field distribution and the light interference pattern. It results directly from the transport of the photoinduced carriers during the grating formation. This phase shift Ψ is given by

$$\Psi=\arctan\left[\frac{E_D}{E_0}\left[1+\frac{E_D}{E_q}+\frac{E_0^2}{E_DE_q}\right]\right] . \tag{5}$$

Equation (5) shows that the relative phase between the index grating and the light pattern is a function of the applied field. Without external field applied along the grating vector, the buildup of the photorefractive grating is governed by diffusion, resulting in a space-charge distribution in phase with the light pattern. The phase shift Ψ of the space-charge field and the refractive index grating with respect to the light is then $\pi/2$ since the space-charge distribution and the resulting space-charge field are related through the Poisson equation. When an external field is applied, the buildup of the space-charge distribution is also governed by drift. The dephasing Ψ between the space-charge field and the light is then given by Eq. (5).

In photoconductive polymers, the photogeneration of free carriers is strongly electric-field dependent.[8–11] The absorption of a photon leads to the creation of a bound electron-hole pair. The electron and the hole can recombine or can be separated by an externally applied field into a free electron and a free hole. This field-separation process competing with geminate recombination is commonly described by Onsager's theory.[17] This theory gives an expression for the efficiency $\phi(r_0,E)$ of photogeneration of free carriers that participate to charge migration by hopping between adjacent pendant groups of the polymer. An approximation of this Onsager photogeneration efficiency has been given by Mozumder[19] as

$$\phi(r_0,E)=\phi_0\left[1-\zeta^{-1}\sum_{n=0}^{\infty}A_n(\eta)A_n(\zeta)\right] , \tag{6}$$

where $A_n(x)$ is a recursive formula given by

$$A_n(x)=A_{n-1}(x)-\frac{x^n\exp(-x)}{n!} \tag{7}$$

and

$$A_0(x)=1-\exp(-x) . \tag{8}$$

In Eq. (6), ϕ_0 is the primary quantum yield, i.e., the fraction of absorbed photons that results in bound thermalized electron-hole pairs and is considered independent of the applied field E. $\eta=r_c/r_0$ and $\zeta=er_0E/k_BT$ where $r_c=e^2/4\pi\varepsilon_0\varepsilon k_BT$ and r_0 is a parameter that describes the thermalization length between the bound electron and hole. According to this theory, the diffraction efficiency of a photorefractive grating written in polymers with pendant groups will be strongly field dependent since an externally applied field increases the number of photogenerated carriers that migrate by drift and lead to the buildup of the space charge. In our model, to describe the photorefractive effect in polymers, we assume that the space-charge field in these materials is limited by the efficiency of photogeneration of free carriers $\phi(r_0,E)$, rather than by the density of traps N_A. In addition, in poled polymers, the electro-optic coefficient is no longer a

constant of the material as in inorganic crystals, but depends on the external field that is applied for the poling to generate the electro-optic effect. Therefore, r_{eff} in Eq. (1) is field dependent. The applied field then affects the value of the amplitude of the space-charge field, the value of the electro-optic coefficient, and the relative phase between the index grating and the light pattern. Since the dc dielectric constant is lower in organic materials compared to inorganic crystals, the space-charge field amplitudes can reach higher values (>1 V/μ). If such fields are high enough to pole the polymer, the internal space-charge field could interfere with the external poling field and alter the effective electro-optic coefficient. For the polymers discussed here, this effect can be neglected since high poling field are needed to orient the nonlinear chromophores. The electro-optic coefficient is therefore only a function of the external field. Its field dependence is measured by Mach-Zehnder–type interferometric measurements as described in Sec. IV.

III. EXPERIMENTAL METHOD

A. Sample preparation and characterization

To be photorefractive, a polymer must be photoconductive and show the electro-optic effect. Different approaches can be employed to design a functional polymer that fulfills these requirements. Doping of a polymer matrix with a photosensitizer, a transport agent, or nonlinear chromophores has been employed so far.[3,5] This guest-host approach leads to materials with a low glass transition temperature T_g and is limited by the relatively low concentrations of dopants that can be mixed into the polymer matrix. Our strategy for the design of a photorefractive polymer was to start from polyvinylcarbazole (PVK) which is well known for its photoconductive properties and to modify it to also become electro-optic. We synthesized[7] a methacrylic ester polymer containing carbazole groups attached as a side chain to the polymer backbone with an alkylene spacer. This polymer was reacted with tetracyanoethylene which transformed some of the carbazole groups into tricyanovinylcarbazole groups (TCVK). The chemical structure of the polymer is shown in Fig. 1(a). The carbazole group has a long π conjugation along the two aromatic rings; the nitrogen atom in the carbazole group is an electron donor, while the tricyanovinyl group is an electron acceptor. Tricyanovinylcarbazole is a moiety with a donor-acceptor group and has, therefore, second-order optical nonlinearities. The advantage of this approach is that one can get polymeric systems with a higher T_g and consequently a higher poling stability. But in return for better stability, higher poling fields are needed causing difficulties during the poling process of thick samples. This approach also offers flexibility as T_g can be varied by changing the polymer backbone, or the spacer group, or by adding a plasticizer. The high-T_g (95 °C–100 °C) polymer shown in Fig. 1(a) was modified into the low-T_g (room-temperature) polymer shown in Fig. 1(b). The backbone was changed from methacrylate to acrylate and benzylbutylphthalate was added as a plasticizer. The acrylate polymer with

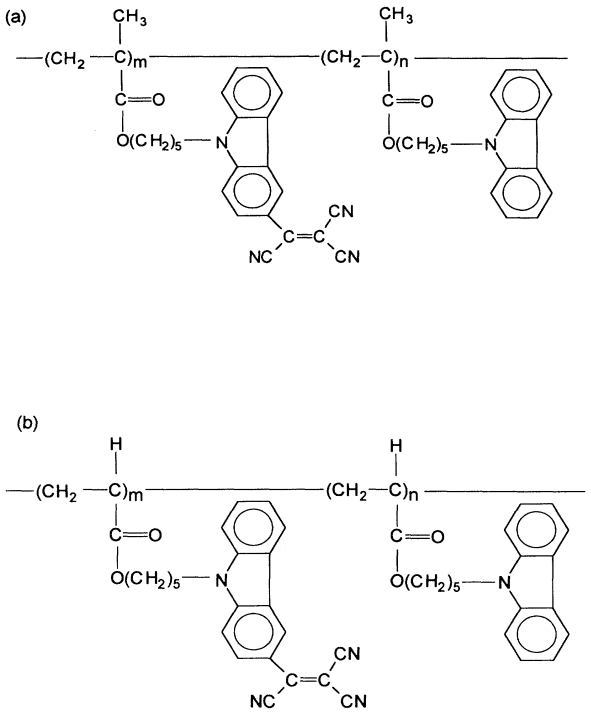

FIG. 1. Structure of the carbazole-tricyanovinylcarbazole (PVK-TCVK) polymer. (a) Methacrylate form, (b) acrylate form.

plasticizer was used to fabricate thick samples (~ 100 μm) for the photorefractive experiments since poling in these samples is easier than in the methacrylate polymer samples. Thin samples, obtained by spin coating the methacrylate polymer (high-T_g) on indium-tin-oxide (ITO) glass, showed a strong electro-optic effect with good stability after a poling field of 100 V/μm was applied. An electro-optic coefficient of $r_{33}=6$ pm/V was measured at 830 nm in a 3-μm-thick film. It has been shown[7] that 75% of the initial poling value of the electro-optic was maintained for more than 380 h after poling. The photoconductivity was also studied[7] by measuring the photocurrent through thin high-T_g samples. A dielectric constant of $\varepsilon=3.9$ and a refractive index of $n=1.67$ were determined.

The linear absorption spectrum of the PVK-TCVK polymer is shown in Fig. 2. It shows a broad absorption band centered around 500 nm which is due to the charge-transfer absorption. The methacrylate and acrylate forms of the polymer have similar optical properties in the visible spectrum. The inset of Fig. 2 depicts the absorption spectrum of a 100-μm-thick sample. At 700 nm, where the wave mixing experiments were performed, the optical density is around 0.5. For the experiments presented here, the polymer was sandwiched between two ITO glass slides and filled a circular window cut in a Teflon film which was used as a spacer. Teflon has good electrical insulating properties and reduces the breakdown problems that might occur when a high electric field is applied across the sandwich.

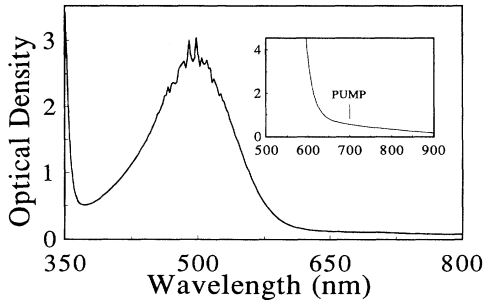

FIG. 2. Linear absorption spectrum of a 2-μm-thin PVK-TCVK polymer film. Inset: linear absorption spectrum of a 100-μm-thick sample.

B. Experimental setup

To establish and study the photorefractive effect in our polymeric system, we performed backward degenerate four-wave-mixing experiments and Mach-Zehnder–type interferometric measurements for an independent characterization of the electro-optic properties.

The Mach-Zehnder interferometric apparatus[20] is shown in Fig. 3. The intensity at the output of the interferometer is given by

$$I=\tfrac{1}{2}[E_1^2+E_2^2+2E_1E_2\cos(\phi_2-\phi_1)] , \tag{9}$$

where E_i are the field amplitudes of the light in each arm of the interferometer and $\phi_2-\phi_1$ is their relative phase. If an electric field with frequency Ω is applied to the electro-optic sample which is placed in one arm of the interferometer, the relative phase will be modulated as

$$\phi_2-\phi_1=\phi_0+A\cos(\Omega t) , \tag{10}$$

where ϕ_0 is the relative phase without electro-optic modulation. A is the modulation amplitude given by

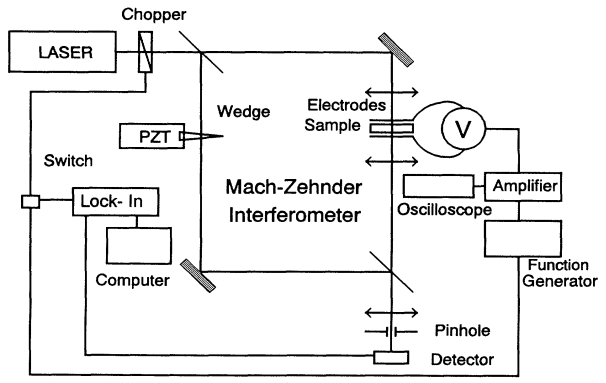

FIG. 3. Schematic representation of the interferometric Mach-Zehnder setup used for the measurement of the electro-optic coefficient.

$$A=\pi r_{13}n^3V/\lambda . \tag{11}$$

λ is the wavelength of the light, n the refractive index at λ, r_{13} the electro-optic coefficient, and V is the amplitude of the applied voltage. Substituting Eq. (10) into Eq. (9), we see that the modulated signal $\Phi(\Omega)$ of the interferometer is given by

$$\Phi(\Omega)=E_1E_2\cos[\phi_0+A\cos(\Omega t)] . \tag{12}$$

Since the modulation amplitude A is small, the right-hand side of Eq. (12) can be expanded in A and the interferogram modulation at the frequency Ω simplifies into the first order of A to

$$\Phi(\Omega)=-E_1E_2A\sin(\phi_0)\cos(\Omega t) . \tag{13}$$

The intensity at the output of the interferometer is therefore modulated at frequency Ω with an amplitude that depends on the product of the field amplitudes E_1E_2, on the amplitude A, and on the relative phase ϕ_0 of the interferometer when no electro-optic modulation is applied to the sample. The product E_1E_2 can be determined independently by measuring the intensity modulation of the interferometer when only the reference arm is modulated. This is done in our case by a wedge mounted on a PZT crystal driven by a sawtooth signal such that the relative phase is changed by π several times. In this case, the maximum $I_{\max}$ and the minimum $I_{\min}$ intensities which are detected are related to E_1E_2 by

$$E_1E_2=\tfrac{1}{2}(I_{\max}-I_{\min}) . \tag{14}$$

For this measurement, the s-polarized light is chopped and the output intensity is measured with the lock-in amplifier at the chopper frequency. Since the chopped signal has a squared wave form, the total amplitude measured with the lock-in is half the real amplitude modulation that appears in Eq. (14). To determine A from Eq. (13) we need the value of ϕ_0. The latter is changed continuously with the wedge placed in the reference arm, so that the signal detected with the lock-in at frequency Ω is modulated by the factor $\sin(\phi_0)$ in Eq. (13). In this case, the results are not influenced by an undesired change of ϕ_0 that could occur during the experiment. Substituting Eqs. (11) and (14) into Eq. (13), the electro-optic coefficient can be determined from

$$r_{13}=\frac{\lambda}{\pi n^3V^{\rm rms}}\frac{I_s^{\rm rms}(\Omega)}{I_{\max}-I_{\min}} , \tag{15}$$

where $I_S^{\rm rms}(\Omega)$ is the amplitude of the modulation of the intensity at the frequency Ω at the output of the interferometer. Our experiments were carried out at $\lambda=632.8$ nm. A sinusoidal signal with a frequency $\Omega\approx1$ kHz and an amplitude of the order of $V^{\rm rms}=20$–40 V which was superimposed on a dc part ranging from 0 to 2000 V was applied across the sample. The dc part of the applied field poles the polymer and induces the electro-optic effect. It could be switched on and off independently of the sinusoidal part so that the dynamics of the pol-

ing could be studied *in situ*.

The backward degenerate four-wave-mixing experiments were performed in a tilted configuration. Two pump beams labeled I_1 and I_2 impinged onto the sample with an angle of α_1 and α_2 with respect to the normal to the sample (measured inside the sample with $\alpha_2 > \alpha_1 > 0$). The tilted configuration is shown in Fig. 4. In this configuration, the external field had a component E_0 along the direction of the grating vector **K** given by $E_0 = V_{ext} \sin(\beta)/d$ where β is the slant angle of the grating $[\beta = (\alpha_1 + \alpha_2)/2]$. V_{ext} is the external voltage applied to the sample, and d is the thickness of the sample. The grating spacing Λ is then given by $\Lambda = \lambda/2n \sin[(\alpha_2 - \alpha_1)/2]$. A much weaker third beam I_3 was counterpropagating with respect to beam I_1 with p polarization as opposed to the pump beams which were s polarized. The diffracted signal I_4 was counterpropagating with respect to I_2 and its intensity was measured with an amplified Si photodiode and a lock-in amplifier with the probe beam I_3 being chopped at 1 kHz. The diffracted signal was continuously detected over periods of time as long as 600 s and was divided by a reference signal. The laser source was a cw Pyridine 2 dye laser pumped by an Ar laser. The intensities of our pump beams were in the range of 10 to 20 mW corresponding to a power density of 0.3 to 0.6 W/cm^2. The ratio of the intensities of the two pump beams was adjusted in order to account for the Fresnel losses of each pump beam on the entrance glass slide of the sample.

IV. RESULTS AND DISCUSSION

A. Electro-optic effect

In polymers, the orientational averaging of the second-order molecules leads to a macroscopic cancellation of the nonlinear contribution from individual molecular constituents. To show an electro-optic effect, the polymeric samples need to be oriented under a dc poling field. This poling process induces a polar axis in the polymer. The class of symmetry[21] is ∞mm. The electro-optic tensor has only two independent tensor elements: r_{33} along the poling direction and r_{13} in any perpendicular direction. It is generally accepted[22] that r_{33} is three times larger than r_{13}. Since the poling field is applied between the two ITO glass slides, the polar axis is perpendicular to the plane of the polymer sample. In low-T_g polymers, the generation of an electro-optic coefficient through poling can be studied *in situ* at room temperature with the Mach-Zehnder interferometer described in Sec. III A. Figure 5 shows the amplitude of the modulated signal $I_S(\Omega, t)$ at the output of the interferometer. According to Eq. (15) this amplitude is proportional to the electro-optic coefficient r_{13}. At $t = 66$ s, a dc voltage of 1.5 kV is superposed to a sinusoidal voltage $V^{rms} = 33.7$ V. The amplitude of the modulated signal increases rapidly to a higher value due to poling of the sample. The high-frequency modulation of the signal is the result of the periodic tuning of the relative phase in the reference arm of the interferometer with the wedge mounted on a PZT. When the dc part of the applied field is switched off, the electro-optic effect vanishes rapidly to its initial value at $t < 66$ s. Figure 5 shows that the polymer undergoes a rapid loss of its electro-optic properties after the poling field is switched off but that a residual poling stays for longer times. The magnitude of the residual poling is $r_{13} = 0.07$ pm/V. At time $t = 300$ s, the sinusoidal voltage is switched off; there is no longer electro-optic phase modulation and the signal goes down to the noise level of the experiment. Figure 6 shows the values of the electro-optic coefficient r_{13} obtained with this technique, as a function of the applied dc voltage in a 75-μm-thick sample. It shows that in the range of a dc poling voltage V_{ext} of 0 to 2000 V, the electro-optic response is almost proportional to the applied voltage. If we assume that the poling field is given by $E_{ext} = V_{ext}/d$, where d is the thickness of the sample, we get a value of $r_{33} = 3r_{13} = 0.63 \pm 0.06$ pm/V for a poling field of $E_{ext} = 20$ V/μm. This value is small compared to the one we measured in 2-μm-thick thin spin-coated samples but the value of the poling field is one order of magnitude lower. Higher values of the electro-optic coefficient could be reached if higher voltages could be applied to thick samples without facing the problem of electrical breakdown through the sample. To improve the poling process it is important to improve the quality of the films. The formation of pinholes during the sample fabrication

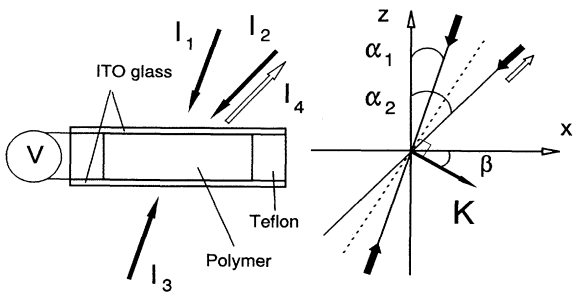

FIG. 4. Tilted configuration used in the backward degenerate four-wave-mixing experiments.

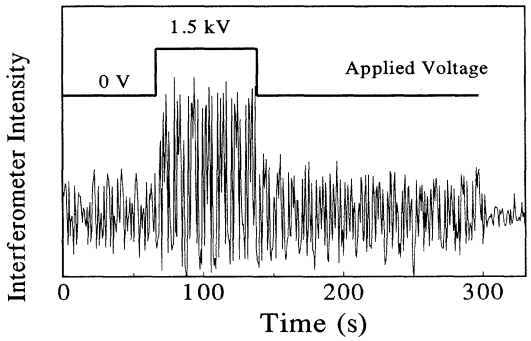

FIG. 5. Dynamics of the poling of a low-T_g acrylate PVK-TCVK polymer sample measured *in situ* with the Mach-Zehnder interferometer.

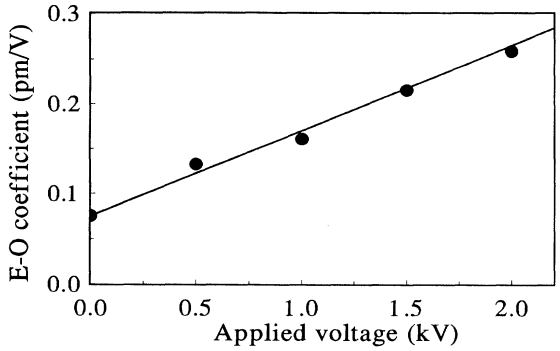

FIG. 6. Electro-optic coefficient r_{13} as a function of the applied voltage measured in a low-T_g acrylate PVK-TCVK polymer sample.

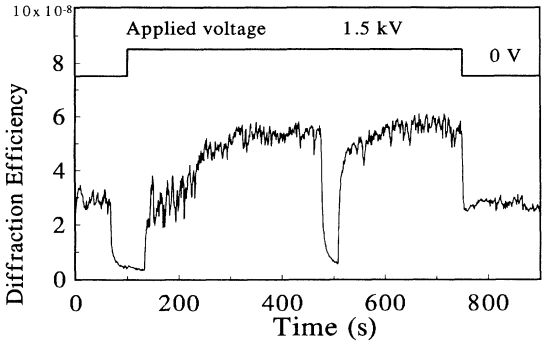

FIG. 7. Diffraction efficiency versus time showing evidence for an absorptive grating and an electro-optic photorefractive grating when an external poling field is applied. Both gratings have erase-write properties ($\lambda = 700$ nm, $d = 100$ μm).

reduces considerably the value of the poling field that can be applied across the sample. Poling in vacuum could also improve the electro-optic properties of thicker samples.

B. Four-wave-mixing experiments

We will now present the results of the four-wave-mixing experiments. We first discuss photorefractive and absorptive gratings written at 700 nm in 70–150-μm-thick samples. These gratings are erasable and have to be distinguished from other permanent gratings due to photochemical reactions of the polymer when it is excited close to its absorption band centered at 500 nm. Such photobleaching effects will be discussed at the end of this section.

In the tilted configuration described previously in Sec. III B and shown in Fig. 4, we measure the diffracted signal as a function of the voltage V_{ext} applied across the sample. This applied voltage induces the electro-optic effect in the sample, helps for the generation of photocarriers, and helps in the buildup of the photorefractive space-charge distribution as a drift source. Figure 7 shows the diffraction efficiency versus time in a 100-μm-thick sample oriented such that $\alpha_2 = +31°$ and $\alpha_1 = +17°$. The value of the grating spacing corresponding to this configuration is $\Lambda = 1.7$ μm. The value of the slant angle β is 25°. At $t = 0$ s, without bias field ($V_{\text{ext}} = 0$), a grating is detected whose diffraction efficiency is $\eta = 3 \times 10^{-8}$. This signal can be erased, as evidenced by blocking the beam I_1 at $t = 66$ s. Without poling field the polymer is almost isotropic and shows only a residual electro-optic effect. This zero-field electro-optic effect is too small to generate an electro-optic photorefractive grating with such a diffraction efficiency. We attribute this signal to the absorption grating resulting from the periodic light distribution and the corresponding absorption changes between the dark and light regions. The origin of these gratings is not well understood yet. However, they have to be distinguished from thermal gratings and permanent gratings that could be induced by photochemical effects.

As depicted in Fig. 7, when an external voltage of 1.5 kV is applied across the sample for poling and when the second pump beam is restored, the diffraction efficiency increases by a factor of 2 compared to the diffraction efficiency measured without the field. This diffracted signal is due to the formation of an electro-optic photorefractive grating superimposed on the absorptive grating discussed previously. The dynamics of the buildup of the photorefractive gratings is complex and shows different time constants. At $t = 475$ s, one of the pump beam is blocked and the signal vanishes. The uniform light illumination of a single pump beam erases the periodic space-charge distribution previously written in the material by the two interfering pump beams. The signal vanishes since both photorefractive and absorptive contributions are erased. In the presence of the two pump beams ($t = 510$ s) a new periodic space-charge distribution is written in the material and the diffracted signal grows to reach its former steady-state value. When the applied voltage is removed at $t = 750$ s, the electro-optic effect is lost and the signal decreases rapidly reaching its steady-state value when only the absorptive contribution is present. The dynamics of this process is consistent with the dynamics of the loss of the electro-optic effect measured with the Mach-Zehnder interferometer and is discussed in Sec. IV A. Within the time resolution of our experimental apparatus (0.3 s), the erase-write dynamics is independent of the applied field. On the time scale of our experiments, absorptive and photorefractive gratings show the same erase-write dynamics. Figure 8(a) shows an erase-write process. The dynamics is compared to the standard Kukhtarev model.[23] In this model, the diffraction efficiency $\eta_e(t)$ during the erasure of the grating and the diffraction efficiency $\eta_w(t)$ during the writing of the grating are given by

$$\eta_e(t) \propto [\exp -(t - t_e)/\tau]^2 , \tag{16a}$$

$$\eta_w(t) \propto [1 - \exp -(t - t_w)/\tau]^2 . \tag{16b}$$

τ is the time constant, and t_e and t_w are the times when

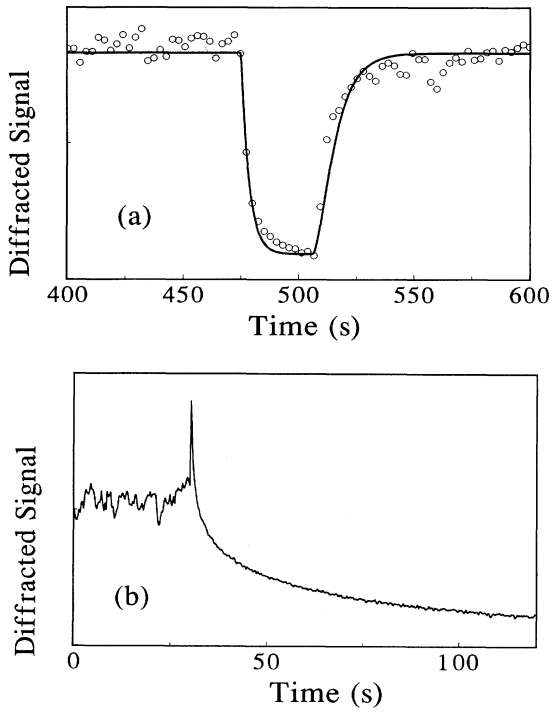

FIG. 8. (a) Erase and write dynamics of the photorefractive grating. Circles: experimental points; full line: theoretical fit. At $t=475$ s one of the pump beams was blocked and the signal vanishes. At $t=510$ s, both pump beams are present. (b) Storage time of the space-charge distribution measured when both pump beams are blocked.

one of the pump beam is blocked and restored, respectively. As shown in Fig. 8(a) (full line), the best fit gives a time constant of $\tau=7$ s for pump beams with a power density of 0.4 W/cm^2. The fit is not completely satisfactory, indicating that the buildup of the grating is a more complex process. Figure 8(b) shows the decay of the diffraction efficiency when both pump beams are blocked. This decay measures the storage time of the grating and is longer than the erasure process when only one pump beam in blocked. The storage time is mainly limited by the lifetime of the trapped carriers.

In the backward degenerate four-wave-mixing configuration, the diffraction efficiency η can be approximated as[24,25]

$$\eta=\exp\left[\frac{-\alpha d}{(\cos\alpha_1\cos\alpha_2)^{1/2}}\right]\left[\frac{\pi\Delta\tilde{n}d(\hat{\mathbf{e}}_i\hat{\mathbf{e}}_d)}{\lambda(\cos\alpha_1\cos\alpha_2)^{1/2}}\right]^2, \quad (17)$$

where $\hat{\mathbf{e}}_i$ and $\hat{\mathbf{e}}_d$ are unitary vectors along the polarization of the incident and the diffracted beams, respectively. $\Delta\tilde{n}$ is the complex refractive index variation that contains a refractive index change Δn and an absorption change $\Delta\alpha(\Delta\tilde{n}=\Delta n+i\lambda\Delta\alpha/4\pi)$. The dispersive contribution Δn is the electro-optic effect and is given by Eq. (1). The linear electro-optic Pockels effect is a second-order process due to the mixing of the space-charge field (at zero frequency) and the optical field. The calculation of the effective electro-optic coefficient r_{eff} is analogous to the treatment of second-harmonic generation[26] and is given by

$$r_{\text{eff}}=\hat{\mathbf{e}}_d\cdot\left[\overleftrightarrow{R}:\hat{\mathbf{k}}\cdot\hat{\mathbf{e}}_i\right], \quad (18)$$

where $\hat{\mathbf{k}}$ is a unit vector along the space-charge field (along the grating vector). $\overleftrightarrow{R}$ is the electro-optic tensor with the symmetry of poled polymers.[21,22] The x,y,z axes system is defined such that the z direction is pointing in the direction perpendicular to the surface of the sample and the x,y plane defines the surface of the sample. In our tilted configuration and for a readout of the grating with p-polarized light, we have $\hat{\mathbf{e}}_d=(\cos\alpha_2,0,\sin\alpha_2)$, $\hat{\mathbf{e}}_i=(\cos\alpha_1,0,\sin\alpha_1)$, and $\hat{\mathbf{k}}=(\cos\beta,0,\sin\beta)$ so that Eq. (15) becomes

$$r_{\text{eff}}=r_{13}\cos\alpha_2\sin(\alpha_1+\beta)+r_{13}\sin\alpha_2\cos\alpha_1\cos\beta+r_{33}\sin\alpha_1\sin\alpha_2\sin\beta\,. \quad (19)$$

In this calculation, we neglect the anisotropy of the refractive index in the sample. The experimental points in Fig. 9 show the steady-state diffraction efficiency measured in a 75-μm-thick sample at 715 nm as a function of the applied voltage. The strong field dependence of the signal is the signature of the photorefractive effect. To fit the total diffraction efficiency we apply Eq. (17) under our experimental conditions. Both the absorptive and the photorefractive contributions are taken into account. Therefore, in Eq. (17) the amplitude of the complex refractive index $\Delta\tilde{n}$ is given by

$$\Delta\tilde{n}(x,E_0)=\Delta n(E_0)\sin[Kx+\Psi(E_0)]+\frac{\Delta\alpha\lambda}{4\pi}\cos(Kx)\,. \quad (20)$$

$\Delta n(E_0)$ is given by Eqs. (1), (2), and (19). The field dependence of the electro-optic tensor elements is measured independently by the electro-optic measurements described in Sec. IV A. It is fitted by the liner function $r_{13}(V_{\text{ext}})=aV_{\text{ext}}+b$. In the sample for which wave mix-

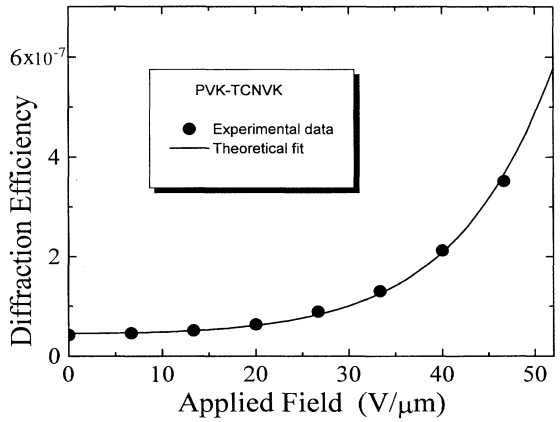

FIG. 9. Electric-field dependence of the total diffraction efficiency in the photorefractive system. Circles: experimental points; full line: theoretical fit using a modified Kukhtarev model.

ing results are presented in Fig. 9, we measured $a=9.15\times10^{-5}$ pm V^{-2}, $b=7.5\times10^{-2}$ pm V^{-1}. This linear dependence is shown by the straight line in Fig. 6. The best fit to the field-dependent diffraction efficiency measured in our poled polymers is shown by the full line curve in Fig. 9. It has been obtained using Eqs. (1)–(5), (17), (19), and (20). The trap density N_A appearing in Eq. (4) was replaced by N_{PC} the density of photogenerated free carriers which is given by

$$N_{PC}=\frac{I\alpha\tau}{\hbar\omega}\phi(r_0,E)\ , \tag{21}$$

where I is the power density in the maxima of the light modulation, α is the absorption coefficient, τ the lifetime of the carriers, and $\hbar\omega$ is the photon energy. The Onsager efficiency for photogeneration $\phi(r_0,E)$ is given by Eq. (6). The configuration was $\alpha_1=+9°$ and $\alpha_2=+25°$ (angles inside the sample) leading to a slant angle $\beta=17°$ and a grating spacing of $\Lambda=1.5$ μm. At 300 K, the diffusion field is $E_D=0.1$ V/μm and the space-charge field is $E_{sc}=0.2$ V/μm for an applied voltage of 1000 V. The absorbance of the sample at 715 nm was $\alpha d=0.69$. The best fit was obtained with $\tau=60$ s, $r_0=1.63$ nm and $\phi_0=1.6\times10^{-6}$. In Eq. (6) the infinite sum was truncated at $n=10$ where good convergence was found. These calculations show that the simple Kukhtarev model, modified to take into account the field dependence of the electro-optic coefficient and the field-dependent Onsager photogeneration efficiency, gives in first approximation a satisfactory description of the photorefractive effect in our poled polymers.

The photorefractive gratings discussed previously have to be distinguished from other possible gratings such as thermal and photochemical ones. The dynamics of the gratings detected in our experiments is too slow to be compatible with a thermal grating.[25] The physical constants (density, specific-heat capacity, and heat conductivity) of methacrylate polymers would lead to a typical time constant of a few microseconds for the dynamics of thermal grating formation in these materials. Indeed, we detected some permanent gratings when the polymer was excited close to its absorption band centered at 500 nm. Beam-coupling experiments[2] showed that under resonant excitation the polymer undergoes a permanent partial bleaching of its absorption band and related refractive index changes which are attributed to a photochemical reaction of the polymer. A refractive index change of $\Delta n=-0.002$ was measured in a 2-μm-thick film after an exposure to two interfering pump beams with a power density of 0.5 W/cm^2 at 600 nm for 15 min. The high refractive index changes they induce at this wavelength hide any photorefractive signal. Close to its absorption band, the polymer shows the highest photogeneration which is suitable for the photorefractive effect, but on the other hand, it experiences also these photobleaching effects. The choice of the excitation wavelength for the photorefractive effect is therefore a trade off between good photosensitivity and good photochemical stability. The photosensitivity can be increased at longer wavelength where the polymer does not show photobleaching effects, by adding a photosensitizer to the polymeric system.[27] Nevertheless, the permanent photobleaching is an interesting property that can be used to write waveguide structures with photolithography masks and UV light exposure.

V. CONCLUSION

In summary, the photorefractive effect has been evidenced and studied in the PVK-TCVK polymeric system. This is the first report of photorefractivity in a side chain polymeric system. We showed that the field-dependent electro-optic photorefractive effect is accompanied by an absorptive contribution. The absorptive effect is dominant in the absence of any external electric field. To describe photorefractivity in these materials, we applied the steady-state Kukhtarev model modified to describe the field dependence of the electro-optic coefficient occurring in low-T_g poled polymers and the field-dependent Onsager photogeneration efficiency. The model gives a good description of the diffraction efficiency measured for different values of the applied field. It shows that a good photogeneration efficiency is the basic key to get high diffraction efficiencies. A better understanding of the microscopic mechanisms has to be established in order to further improve the theoretical description of this new class of materials. In this study, we established the photorefractivity in the acrylate form of the PVK-TCVK system. This material has a low T_g and consequently a low poling stability but in exchange can be poled more easily than the methacrylate form which has a high T_g and a good stability. At this point, the material has also a slow speed (several seconds) limited by low mobilities. Molecularly doping of this material through fullerene doping,[6,28] for instance, or by adding trinitrofluorenone[8–10] which forms an efficient charge transfer complex with PVK could improve the efficiency of photocarrier generation and therefore increase the diffraction efficiency and the speed of these new materials.

ACKNOWLEDGMENTS

The authors would like to acknowledge support from the NSF (Grant No. ECS-89-11960), AFOSR (Grant No. 92-NC-260), and the Optical Circuitry Cooperative of the University of Arizona. One of the authors (B.K.) acknowledges support from NATO.

*Permanent address: Institut de Physique et Chimie des Matériaux, Strasbourg, France.
†Present address: Toray Industries, Inc., Sonoyama, Otsu, Shiga, Japan.

[1] *Photorefractive Materials and Their Applications,* edited by P. Günter and J. P. Huignard (Springer-Verlag, Berlin, 1988), Vols. I and II.
[2] K. Sutter and P. Günter, J. Opt. Soc. Am. B 7, 2274 (1990).

[3]S. Ducharme, J. C. Scott, R. J. Twieg, and W. E. Moerner, Phys. Rev. Lett. **66**, 1846 (1991).
[4]S. M. Silence, C. A. Walsh, J. C. Scott, T. J. Matray, R. J. Twieg, F. Hache, G. C. Bjorklund, and W. E. Moerner, Opt. Lett. **17**, 1107 (1992).
[5]Y. Cui, Y. Zhang, P. N. Prasad, J. S. Schildkraut, and D. J. Williams, Appl. Phys. Lett. **61**, 2132 (1992).
[6]Y. Zhang, Y. Cui, and P. N. Prasad, Phys. Rev. B **46**, 9900 (1992).
[7]K. Tamura, A. B. Padias, H. K. Hall, Jr., and N. Peyghambarian, Appl. Phys. Lett. **60**, 1803 (1992).
[8]M. Stolka, in *Encylopedia of Polymer Science and Engineering,* edited by H. F. Mark and J. I. Kroschwitz (Wiley, New York, 1988), Vol. 11, p. 154.
[9]W. D. Gill, J. Appl. Phys. **43**, 5033 (1972).
[10]J. Mort, Adv. Phys. **29**, 367 (1980).
[11]P. M. Borsenberger and A. I. Ateya, J. Appl. Phys. **49**, 4035 (1978).
[12]V. L. Vinetskii and N. V. Kukhtarev, Fiz. Tverd. Tela (Leningrad) **16**, 3714 (1975) [Sov. Phys. Solid State **16**, 2414 (1975)].
[13]N. V. Kukhtarev, Pis'ma Zh. Tekh. Fiz. **2**, 1114 (1976) [Sov. Tech. Phys. Lett. **2**, 438 (1976)].
[14]N. Kukhtarev, V. Markov, and S. Odulov, Opt. Commun. **23**, 338 (1977).
[15]V. L. Vinetskii and N. V. Kukhtarev, Kvant. Elektron. (Moscow) **5**, 405 (1978) [Sov. J. Quantum Electron. **8**, 231 (1978)].
[16]N. V. Kukhtarev, V. B. Markov, S. G. Odulov, M. S. Soskin, and V. L. Vinetskii, Ferroelectrics **22**, 949 (1979).
[17]L. Onsager, Phys. Rev. **54**, 554 (1938).
[18]A. Twarowski, J. Appl. Phys **65**, 2833 (1989).
[19]A. Mozumder, J. Chem. Phys. **60**, 4300 (1974).
[20]K. D. Singer, M. G. Kuzyk, W. R. Holland, J. E. Sohn, S. J. Lalama, R. B. Comizzoli, H. E. Katz, and M. L. Schilling, Appl. Phys. Lett. **53**, 1800 (1988).
[21]P. N. Prasad and D. J. Williams, *Introduction to Nonliner Optical Effects in Molecules and Polymers* (Wiley, New York, 1991).
[22]D. J. Williams, in *Nonlinear Optical Properties of Organic Molecules and Crystals,* edited by D. S. Chemla and J. Zyss (Academic, New York, 1987), p. 405.
[23]G. C. Valley and M. B. Klein, Opt. Eng. **22**, 705 (1983).
[24]H. Kogelnik, Bell Syst. Tech. J. **48**, 2909 (1969).
[25]H. J. Eichler, P. Günter, and D. W. Pohl, in *Laser-Induced Dynamic Gratings,* Springer Series in Optical Sciences Vol. 50 (Springer-Verlag, Berlin, 1986).
[26]G. D. Boyd and D. A. Kleinman, J. Appl. Phys. **39**, 3597 (1968).
[27]N. Peyghambarian, K. Tamura, B. Kippelen, Y. Kawabe, F. Jarka, S. Mazumdar, D. D. Guo, H. K. Hall, Jr., and A. B. Padias, in *Macromolecular Host-Guest Complexes: Optical and Optoelectronic Properties and Applications,* MRS Symposia Proceedings No. 277 (Materials Research Society, Pittsburgh, 1992), p. 145.
[28]Y. Wang, Nature **356**, 585 (1992).